Potential Energy Function and Vibrational States of the Electronic Ground State of N_4^+

Celine Léonard and Pavel Rosmus*

Theoretical Chemistry Group, Université de Marne-la-Vallée, F-77454 Champs-sur-Marne, France

Stuart Carter and Nicholas C. Handy

Department of Chemistry, University of Cambridge, Cambridge, CB2 1EW, United Kingdom

Received: October 13, 1998; In Final Form: December 23, 1998

Three different six-dimensional potential energy functions for the electronic ground state $X^2\Sigma_u^+$ of the N_4^+ have been generated by the RCCSD-T method and the B3LYP and B97-1 density functional approaches. The potentials in their analytic forms have been used in variational calculations of the vibrational states ($J = 0$ and 1). The RCCSD-T rotational B_0 constant of 0.1117 cm^{-1} is in excellent agreement with the experimental value of 0.11205 cm^{-1}. The anharmonic wavenumbers for the fundamentals have been calculated to be $\nu_1 = 2275.6$, $\nu_2 = 390.3$, $\nu_3 = 2239.3$ (expt: 2234.5084), $\nu_4 = 90.7$, and $\nu_5 = 133.8$, and the zero-point vibrational energy is 2675.3 (all values in cm^{-1}). All large isotope shifts observed in a cold matrix for ν_1 and ν_3 have been very well reproduced. Both density functional approaches yielded good agreement for bending fundamentals but failed to desribe accurately the symmetric and antisymmetric stretching vibrations. The dissociation energy, the quadrupole moment and the dipole polarizabilities have been evaluated as well.

1. Introduction

The N_4^+ radical cation has long been known to be formed in discharges through nitrogen.[1] In the dense regions of the planetary ionospheres[2] it might play a role as an intermediate, which, however, will react very rapidly with other species. The electronic ground state of N_4^+ has a linear centrosymmetric equilibrium structure with $^2\Sigma_u^+$ electronic symmetry, as found experimentally in an electron spin resonance study of Knight et al.,[3] in an infrared matrix study of Thompson and Jacox,[4] and in gas-phase rotationally resolved infrared spectrum of Ruchti et al.[5] The photoelectron spectrum of the $(N_2)_2$ cluster measured by Carnovale et al.[6] shows two broad peaks. No bound−bound electronic transitions of N_4^+ have yet been detected. Smith and Lee[7] observed a photodissociation threshold for N_4^+ near 650 nm, with a steady rise of the cross sections until 350 nm. Later, this study has been extended by Ostander and Weisshaar[8] until 270 nm. The unstructured photodissociation spectra show a maximum near 330 nm. Bieske[9,10] studied the photofragmentation of N_4^+ by observing the yield of the fragments' charge-transfer reaction with Ar and the photodissociation of the $(N_2)_n^+$ clusters. The photoion−photoelectron coincidence spectra have been measured by Norwood, Luo, and Ng.[11] The dissociation energy N_4^+ ($X\ ^2\Sigma_u^+$) → N_2 ($X^1\Sigma_g^+$) + N_2^+ ($X^2\Sigma_u^+$) is only slightly higher than 1 eV.[1,11,12] For the electronic ground state more experimental information has been reported concerning the magnetic parameters,[3] the structure,[5] and the streching vibrational transitions.[4,5] The matrix infrared study[4] of the asymmetrically substituted isotopomers of N_4^+ allowed the determination of the energetic position of the antisymmetric and symmetric stretching fundamentals, which lie in $^{14}N_4^+$ at 2271 and 2237 cm^{-1}, and based on harmonic force constants, it has been suggested that the third stretching mode lies between 344 and 480 cm^{-1}.[4] The bending modes have been expected near 100 and 200 cm^{-1}.[13−15] From the gas-phase infrared high-resolution spectrum,[5] an accurate band origin for the antisymmetric stretching vibration has been determined to be 2234.508 cm^{-1} and the rotational constants for the ground and $1\nu_3$ antisymmetric stretch levels have been reported. The magnetic parameters[3] of N_4^+ showed that the unpaired electron resides primarily on the inner nitrogen atoms.

Ab intio calculations[15] predicted that N_4^+ will be a centrosymmetric linear ion before it has been proved experimentally. Later, several other theoretical studies[3,16−19] were published. Hyperfine constants of the EPR spectrum were compared with those calculated from CI wave functions.[3] One-dimensional cuts of the ground and excited state potential energy functions (PEFs) have shown[18] that the low lying electronically excited states will easily dissociate into two diatomic fragments, in accord with experimental findings. So far, only the harmonic wavenumbers have been calculated[19] using the Hartree−Fock approach.

The present study deals with the generation of a six-dimensional PEF for the electronic ground state of N_4^+ and variational calculations of the vibrational states for $J = 0$ and 1 taking the full dimensionality of the problem and the anharmonic effects into account. The goal is to obtain reliable information about the vibrational states of the ion.

2. Generation of the Six-Dimensional Potential Energy Function

The six-dimensional PEFs were mapped by the coupled cluster RCCSD-T approach of Deegan and Knowles[20] using the Dunnings' spdf(vtz) basis set[21] contracted to [4s,3p,2d,1f] for nitrogen, resulting in 120 contracted functions and correlating all valence electrons. This approach yielded excellent[20] spectroscopic constants of the N_2 electronic ground state and was, therefore, chosen for the present study of N_4^+. The electron densities have been calculated from full valence CASSCF wave functions, and the quadrupole moment by the CEPA-1 approach.[22] The computations were done with the MOLPRO program suite,[23] and the difference density plots with the

10.1021/jp984062b CCC: $18.00
Published on Web 03/04/1999

MOLDEN code.[24] For the density functional computations done with the CADPAC program suite,[25] we used the standard B3LYP functional[26] and the newly developed exchange-correlation functional B97-1[27] with the unrestricted HF formalism. In the DFT computations, the tz2p AO basis set with 166 contracted functions has been employed. We refer to the original papers for a detailed description of the methods used to solve the electronic problem. The CPU times per linear geometry were 182 s (B3LYP), 217 s (B97-1) on SG-IP27, and 2056 s (RCCSD-T) on HP-C180, respectively.

The coordinates for the linear centrosymmetric N_4^+ are R_1 and R_2 for the two outer NN bonds, R_3 for the inner bond, ϑ_1 and ϑ_2 for the two bond angles, and τ for the out-of-plane torsion (measured from cis) between the planes $N_1N_2N_3$ and $N_2N_3N_4$.

The energy was calculated at 277 points with RCCSD-T and at 303 or 264 points with the B3LYP and B97-1 approaches, respectively. The PEF has been mapped in the geometry region $80° \le \vartheta_{1,2} \le 180°$, $0° \le \tau \le 360°$, $1.8 \le R_{1,2} \le 2.5$ bohr, and $3.1 \le R_3 \le 5.25$ bohr.

From the calculated energies, a six-dimensional quartic expansion of the PEF of the general form has been generated.

$$V(R_1, R_2, R_3, \vartheta_1, \vartheta_2, \tau) = \Sigma_{ijklmn}\, c_{ijklmn} Q_1^i Q_2^j Q_3^k Q_4^l Q_5^m Q_6^n \quad (1)$$

For the stretches we used the Morse-like coordinate, for the bending, the displacement coordinate, and for the torsion, an even Fourier expansion $Q_6^n = \cos(n\tau)$, reflecting the symmetry of this coordinate:

$$Q_i = 1 - e^{(-0.7(R_i - R_i^{ref}))},\ i = 1,2$$

$$Q_3 = 1 - e^{(-0.73(R_3 - R_3^{ref}))}$$

$$Q_4 = \vartheta_1 - \vartheta_1^{ref}$$

$$Q_5 = \vartheta_2 - \vartheta_2^{ref}$$

$$Q_6^n = \cos(n\tau)$$

The exponents for the Q_i, $i = 1-3$, have been preoptimized in a series of one- and three-dimensional calculations using effective stretch parts of the six-dimensional B3LYP PEF. All potentials have been expanded at the calculated equilibrium geometries (cf. Table 2).

The following restriction in the polynomial expansion was made to fulfill the symmetry conditions defined by Strey and Mills for acetylene:[28] for $n = 0,1$; $i + j + k + l + m \le 4$; with l, m, n of the same parity; for $n = 2$, $l = 2$ and $m = 2$.

Each expansion (1) consisted of 71 coefficients, which are available on our server.[29]

3. Characteristics of the Potential Energy Function and Bonding in N_4^+

In Figure 1, the two-dimensional cuts of the RCCSD-T PEF in the internal coordinates are shown. The PEF is valid up to about 10 000 cm^{-1} above the equilibrium along all internal coordinates. In each cut, there are 41 contours plotted with an interval of 250 cm^{-1}, the remaining coordinates were fixed at their equilibrium values (cf. Table 2). The function reflects the characteristics of the bonding in the ion. The cuts including R_3 are flat along this stretch coordinate, since the two N_2 units are rather weakly bound. Also, the cuts with the bending angles ϑ_1 and ϑ_2 show very flat PEF. Hence, both bending modes and the N···N stretching mode will lie low in energy. Somewhat surprising is the fact that the R_1 vs ϑ_1 and ϑ_2 cuts are almost identical. For the torsion, the cuts with R_1 and R_3 are plotted for $\vartheta_1 = \vartheta_2 = 120°$, and the cut with ϑ_1 for $\vartheta_2 = 120°$. The trans conformation on these cuts is distinctly lower in energy than the cis conformation. The last cut in Figure 1 shows that torsion is only very slightly coupled with ϑ_i.

In Figure 2, two CASSCF difference density plots for the ion at its equilibrium geometry are shown, which help to understand the nature of the bonding. We have chosen two different approaches. In the first one, the total density of the ion has been subtracted from the total density of the neutral van der Waals cluster, and in the second approach, the total density of N_4^+ has been subtracted from the symmetrized total density of the diatoms ($N_2 + N_2^+$). On the left-hand side, the CASSCF electron difference density contour plot $\rho_{N_4} - \rho_{N_4^+}$ is displayed. The regions represented by contours with full lines are those where more electron are present in the ion than in the neutral complex; the broken line contours show the regions with less electrons in the ion. The weak bond between both N_2 units stems mainly from the p_π region. Also, the inner nitrogen atoms have more electrons in the p_π region than in the neutral species. The neon matrix ESR results for N_4^+ showed that the unpaired electron resides primarily on the inner nitrogens but does have an occupancy of about 18% in the $2p_\sigma$ orbital of each terminal atom. From the contour plots, it follows that the s/p_σ region on the inner atoms is very different from the outer atom region. The second plot on the right-hand side of the Figure 2 shows more directly how the N_2 and N_2^+ units form a bond. Again, the electron density in the ion, $\rho_{N_4^+}$, has been taken as a starting point, and with the AO basis set of the tetratomic molecule we have calculated the CASSCF total densities of the N_2 and N_2^+ diatoms. A symmetrized average of the total densities of the diatoms has been subtracted from the total density of the tetratomic ion. The 3D plot shows the surface with 0.0001 e/bohr^3; the broken line is used for the region with an excess of electrons relative to the diatoms average, and the full line for the region with less electrons. Only a small amount of electron density is calculated between both diatoms; the surplus of electrons is found also at the outer atom region, and less electrons are found on the inner nitrogen and in the outer σ region. Both approaches show that the bond between the diatoms is weak and the electron densities at the inner and outer nitrogens are very different.

4. Variational Calculations of the Nuclear Motion Problem

We have used the variational approach described previously for four-atom chain molecules.[30] The kinetic energy operator T_{VR} has been expressed in internal coordinates. The problem of singularities in such an operator while passing from bent to linear structures has been removed by a proper choice of basis functions. Efficient calculation of the matrix elements requires that the PEF is expanded in exactly the same set of coordinates. The computations consist of several steps in which preoptimized contractions for a subsets of the full Hamiltonian are formed. The primitive one-dimensional functions used in these contractions were the eigenfunctions of the Hermite functions for the stretches and Legendre polynomials for the bendings.

The procedure is as follows. A two-dimensional contraction of $(R_1 + R_2)/\sqrt{2}$ and $(R_1 - R_2)/\sqrt{2}$ is first carried out using NBF1 and NBF2 basis functions and M1 and M2 integration points, respectively. From resulting NBF1*NBF2 functions, $NV1(\Sigma_g^+) + NV2(\Sigma_u^+)$ contracted functions are stored. At each

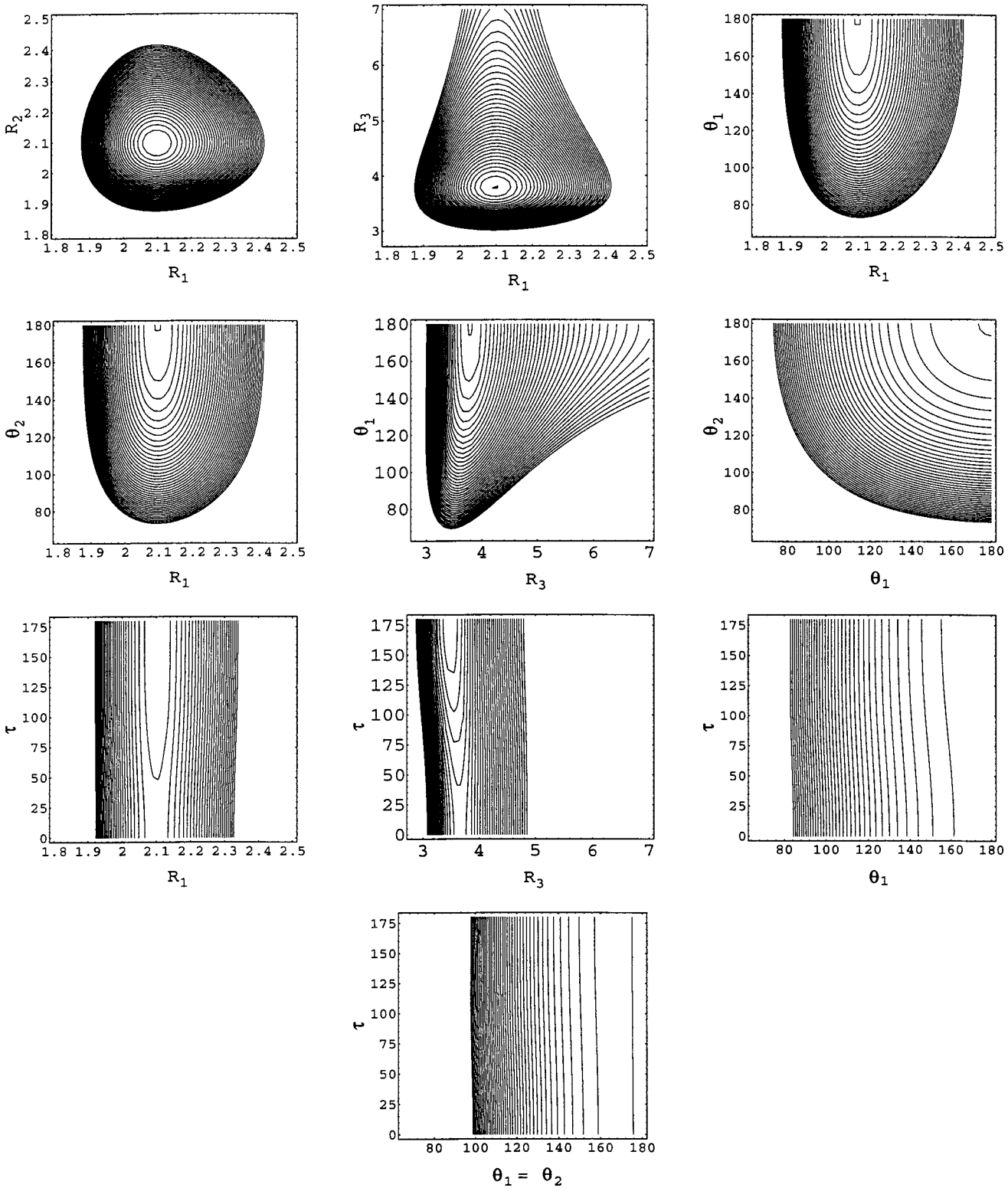

Figure 1. Contour plots of sections of the RCCSD-T PEF for pairs of coordinates defining the six-dimensional expansion. The contour spacing is 250 cm^{-1}; the highest contour is 10 000 cm^{-1}. In the cuts including the torsion and R_1 or R_3, $\vartheta_1 = \vartheta_2 = 120°$, and for τ vs ϑ_1, $\vartheta_2 = 120°$ (R_1, R_2, R_3 are in bohr, and ϑ_1, ϑ_2, τ in degrees).

contraction step, it is ensured that, for example, NBF1 and NBF2 are sufficiently large that the NV1 + NV2 contracted functions are all converged to a required threshold.

These NV1 + NV2 functions in R_1 and R_2 are combined with NBF3 functions in R_3 with M3 integration points, and a further contraction takes place, from which N3D1($\Sigma_g^+ + \Sigma_u^+$) three-dimensional stretch functions are stored from the total of (NV1+NV2)*NBF3. In all the above stretch contraction schemes, the angles are frozen at their equilibrium values.

Turning now to the bending coordinates, a ϑ_1, ϑ_2 contraction (coordinates 4 and 5, respectively) is carried out for two τ (coordinate 6) functions $\cos(0\tau)$ and $\cos(1\tau)$, and then for two τ functions with $\sin(1\tau)$ and $\sin(2\tau)$. These contractions use NBF4 and NBF5 basis functions in θ_1 and θ_2, respectively, with

TABLE 1: Parameters Related to the Basis Set Contractions in the Variational Calculations of the Vibrational States[a]

N3D1 = 30	N3D2 = 40				
NV1 = 16	NV2 = 16	NV4 = 16	NV5 = 16		
NBF1 = 16	NBF2 = 16	NBF3 = 16	NBF4 = 35	NBF5 = 35	NBF6 = 12
M1 = 30	M2 = 30	M3 = 30	M4 = 70	M5 = 70	M6 = 70

[a] For the ^{15}N isotopomers N3D1 = 25 and N3D2 = 30.

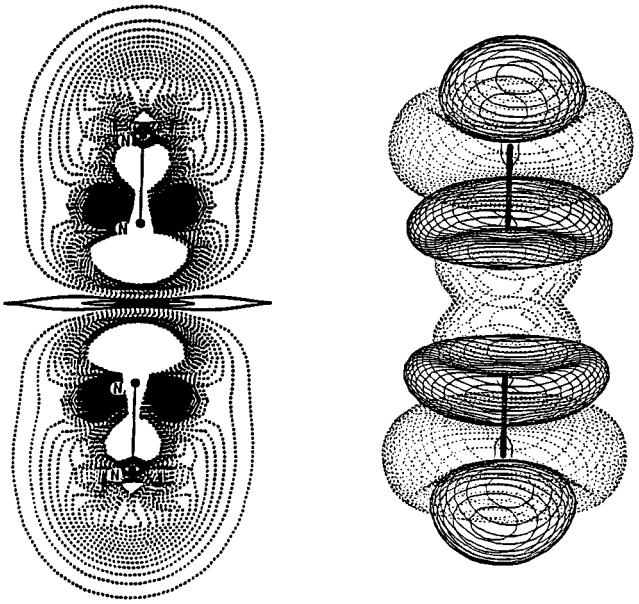

Figure 2. In the left part, the CASSCF difference density contour plot ($\rho_{N_4} - \rho_{N_4^+}$) is displayed. The first contour is drawn for 0.008 e/bohr^3 with steps of 0.008. The full line corresponds to a surplus of electrons, the broken line to the region with less electrons than in N_4. The right-hand side represents a CASSCF surface corresponding to 0.0001 e/bohr^3 in the difference density obtained as a symmetrized average of the N_2, N_2^+, and N_4^+ total densities. The broken line shows the region with more, the full line with less electrons than in the diatoms.

M4 and M5 points, and M6 points are used to integrate the τ integrals. From these NBF4*NBF5 functions, NV4(Σ_g^+) + NV5(Σ_u^+) contracted functions are stored, again ensuring that NBF4 and NBF5 have been set sufficiently high to ensure convergence of the resulting energy levels. These contracted θ functions are then coupled with $(2J + 1)$ rotational functions and NBF6 primitive τ functions in such a way that these θ functions contracted to $\cos(0\tau)$ and $\cos(1\tau)$ give Σ_g^+ and Σ_u^+ functions and those contracted to $\sin(1\tau)$ and $\sin(2\tau)$ give Σ_g^- and Σ_u^- functions. From these (NV4+NV5)*NBF6*(2J+1) functions, N3D2 of each of Σ_g^+, Σ_u^+, Σ_g^-, and Σ_u^- three-dimensional contracted bending functions are stored. In these contractions, the bonds are frozen at their equilibrium values.

The final $J = 0$ and 1 rovibrational energy levels are obtained by combining the N3D1 stretching functions and the N3D2 bending functions with the full Hamiltonian and ensuring that N3D1 and N3D2 are sufficiently large. The values of all the parameters are given in Table 1, which guaranteed the convergence of the calculated $J = 0$ levels presented in this work to within 0.1 cm^{-1}. We refer to ref 30 for a more detailed description of the computational procedure.

5. Results

The results obtained with the B3LYP and B97-1 density functional approaches and the RCCSD-T method are compared in Tables 2 and 3. The latter method yielded excellent spectroscopic constants for N_2 with a vqz(spdfg) basis set.[20] For the six-dimensional PEF of a tetra-atomic molecule, we had to use a smaller vtz(spdf) basis. With this basis, the equilibrium distances for the electronic ground states of the diatoms were calculated to be longer by about 0.01 bohr and the harmonic wavenumber ω_e smaller by 2 cm^{-1} than experiment.[31] Both density functional approaches yielded far too steep PEFs with ω_e larger than experiment by about 80 cm^{-1} and also larger errors in the equilibrium distance by comparison to RCCSD-T.

TABLE 2: Experimental and Calculated Equilibrium Geometries (in bohr), Rotational Constants (in cm^{-1}), and Dissociation Energies (in eV) of the X($^2\Sigma_u^+$) State of N_4^+

method	R_{N-N}	$R_{N\cdots N}$	B_e	B_0	D_e	D_0
B3LYP	2.072	4.048	0.1172[a]	0.1095[b]	1.81	1.77
B97-1	2.078	4.003	0.1182[a]	0.1052[b]	1.83	1.80
RCCSD-T	2.097	3.788	0.1236[a]	0.1117[b]	1.26	1.21
expt[5]				0.11205		
VB[18]	2.03	3.99			1.127	
UMP4[3]	2.058	3.755				
RHF[12]	2.020	3.655			1.42	1.37
RHF[17]	2.092	3.779			1.37	1.31
expt[33]						1.1188 ± 0.0650
expt[9]						1.09 ± 0.08
expt[1]						0.989

[a] Calculated from the equilibrium distances. [b] Calculated from the variational $J = 0$ and $J = 1$ levels.

TABLE 3: Fundamental Vibrational Transitions (in cm^{-1}) and Harmonic Force Constants in Internal Coordinates (in aJ/Å^2)

method	ν_1	ν_2	ν_3	ν_4 (trans)	ν_5 (cis)	F_{N-N}	$F_{N\cdots N}$
B3LYP	2378.0	229.5	2372.4	139.8	95.8	23.89	0.56
B97-1	2350.6	277.1	2326.5	110.5	81.4	23.10	0.56
RCCSD-T	2275.6	390.3	2239.3	133.8	90.7	21.26	1.12
expt[4]	2282.6[a]	344−480[a]	2237.6			20.66	1−2
expt[5]			2234.5				
UHF[19,b]	2322	444.8	2191	225.2	140.2		

[a] Calculated from harmonic force constants.[4] [b] Harmonic wavenumbers.

TABLE 4: RCCSD-T Rotational Energy Levels ($J = 0$ and 1, in cm^{-1}) in the Fundamental Levels of N_4^+

(ν_1,ν_2,ν_3,ν_4^4,ν_5^5)	state	$J = 0$	$J = 1$
(0,0,0,0^0,0^0)	$^2\Sigma_g^+$	0.0	0.223
(0,0,0,0^0,1^1)	$^2\Pi_u^+$		90.711
(0,0,0,1^1,0^0)	$^2\Pi_g^+$		133.845
(0,0,0,0^0,2^0)	$^2\Sigma_g^+$	179.685	179.913
(0,0,0,2^0,0^0)	$^2\Sigma_g^+$	253.295	253.523
(0,1,0,0^0,0^0)	$^2\Sigma_g^+$	390.297	390.519
(0,0,1,0^0,0^0)	$^2\Sigma_u^+$	2239.295	2239.537
(1,0,0,0^0,0^0)	$^2\Sigma_g^+$	2275.575	2275.822

[a] The zero-point vibrational energy G(0,0,0,0^0,0^0) has been calculated to be 2675.3 cm^{-1}.

In Table 2, the calculated equilibrium geometries, rotational constants, and dissociation energies are compared with other theoretical and experimental values. The RCCSD-T rotational constants $B_0 = 0.1117$ cm^{-1} calculated from the energy difference between the variational $J = 0$ and $J = 1$ levels in the vibrational ground state is in an excellent agreement with

TABLE 5: Vibrational Energy Levels (RCCSD-T) of N_4^+ ($X^2\Sigma_u^+$)

$^2\Sigma_g^+$		$^2\Sigma_g^-$	
$(\nu_1,\nu_2,\nu_3,\nu_4^{l_4},\nu_5^{l_5})$	E (cm^{-1})	$(\nu_1,\nu_2,\nu_3,\nu_4^{l_4},\nu_5^{l_5})$	E (cm^{-1})
$(0,0,0,0^0,0^0)$	0.0	$(0,0,0,2^2,2^2)$	462.1
$(0,0,0,0^0,2^0)$	179.7	$(0,0,0,2^2,4^2)$	652.5
$(0,0,0,2^0,0^0)$	253.3		
$(0,0,0,0^0,4^0)$	360.2		
$(0,1,0,0^0,0^0)$	390.3		
$(0,0,0,2^0,2^0)$	444.8		
$(0,0,0,2^2,2^2)$	462.9		
$(0,0,0,4^0,0^0)$	499.6		
$(0,0,0,0^0,6^0)$	541.8		
$(0,1,0,0^0,2^0)$	582.4		
$(0,0,0,2^0,4^0)$	635.3		
$(0,0,0,2^2,4^2)$	654.6		
$(0,1,0,2^0,0^0)$	667.6		
$(1,0,0,0^0,0^0)$	2275.6		
$^2\Sigma_u^+$		$^2\Sigma_u^-$	
$(\nu_1,\nu_2,\nu_3,\nu_4^{l_4},\nu_5^{l_5})$	E (cm^{-1})	$(\nu_1,\nu_2,\nu_3,\nu_4^{l_4},\nu_5^{l_5})$	E (cm^{-1})
$(0,0,0,1^1,1^1)$	228.1	$(0,0,0,1^1,1^1)$	225.0
$(0,0,0,1^1,3^1)$	415.0	$(0,0,0,1^1,3^1)$	409.1
$(0,0,0,3^1,1^1)$	482.0	$(0,0,0,3^1,1^1)$	477.7
$(0,0,0,1^1,5^1)$	602.1	$(0,0,0,1^1,5^1)$	593.7
$(0,1,0,1^1,1^1)$	645.5	$(0,1,0,1^1,1^1)$	642.2
$(0,0,0,3^1,3^1)$	681.8	$(0,0,0,3^1,3^1)$	674.0
$(0,0,1,0^0,0^0)$	2239.3		
$(0,0,1,0^0,2^0)$	2420.5		
$(0,0,1,2^0,0^0)$	2496.0		
$(1,0,0,1^1,1^1)$	2501.1		
$(0,0,1,0^0,4^0)$	2602.3		
$(0,1,1,0^0,0^0)$	2629.4		
$(1,0,0,1^1,3^1)$	2687.8		
$(0,0,1,2^0,2^0)$	2689.6		
$(0,0,1,2^2,2^2)$	2708.1		
$(0,0,1,4^0,0^0)$	2744.8		
$(1,0,0,3^1,1^1)$	2749.3		
$(0,0,1,0^0,6^0)$	2784.9		
$(0,1,1,0^0,2^0)$	2823.1		
$(1,0,0,1^1,5^1)$	2875.7		
$(0,0,1,2^0,4^0)$	2880.8		
$(0,0,1,2^2,4^2)$	2901.0		
$(0,1,1,2^0,0^0)$	2909.5		
$(1,1,0,1^1,1^1)$	2917.7		
$^2\Pi_g$ (trans)		$^2\Pi_u$ (cis)	
$(\nu_1,\nu_2,\nu_3,\nu_4^{l_4},\nu_5^{l_5})$	E (cm^{-1})	$(\nu_1,\nu_2,\nu_3,\nu_4^{l_4},\nu_5^{l_5})$	E (cm^{-1})
$(0,0,0,1^1,0^0)$	133.8	$(0,0,0,0^0,1^1)$	90.7
$(0,0,0,1^1,2^0)$	317.9	$(0,0,0,0^0,3^1)$	270.8
$(0,0,0,1^1,2^2)$	322.6	$(0,0,0,2^0,1^1)$	350.3
$(0,0,0,3^1,0^0)$	380.7	$(0,0,0,2^2,1^1)$	366.0
$(0,0,0,1^1,4^0)$	503.5	$(0,0,0,0^0,5^1)$	452.0
$(0,0,0,1^1,4^2)$	509.8	$(0,1,0,0^0,1^1)$	487.7
$(0,1,0,1^1,0^0)$	545.4	$(0,0,0,2^0,3^1)$	541.4
$(0,0,0,3^1,2^0)$	577.1	$(0,0,0,2^2,3^1)$	557.8
$(0,0,0,3^1,2^2)$	583.1	$(0,0,0,2^2,3^3)$	561.7
$(0,0,0,3^3,2^2)$	607.0	$(0,0,0,4^0,1^1)$	602.8
$(0,0,0,5^1,0^0)$	626.4	$(0,0,0,4^2,1^1)$	615.3
$(0,0,0,1^1,6^0)$	699.0	$(0,0,0,0^0,7^1)$	635.6
		$(1,0,0,0^0,1^1)$	2366.6
		$(0,0,1,1^1,0^0)$	2375.5

the experimental value of 0.11205 cm^{-1}. The $B_{\nu_3=1}$ has been calculated to be 0.1212 cm^{-1}; the experimental value is 0.11176 cm^{-1}. The RCCSD-T equilibrium distances should be rather close to the true R_e values, indicating that the terminal NN bonds are longer than those in the neutral N_2 (2.074 bohr[31]) and slightly shorter than in N_2^+ (2.109 bohr[31]). Both density functional methods underestimate the length of the terminal NN bond and overestimate the length of the inner N···N bond. To date, most of the theoretical studies of the N_4^+ ion used only the Hartree−Fock approximation. All previously calculated SCF dissociation energies (cf. Table 2) were calculated to be not too far off from the experimental values, indicating that the correlation contribution to the dissociation energy into the diatomic fragments is small. Our D_0 RCCSD-T dissociation energy of 1.21 eV, calculated from the difference of total energies of separated diatoms and N_4^+, is probably still too large by about 0.05 eV, but it matches the upper limits of the probably most accurate experimental value.[11]

TABLE 6: Comparison of Experimental and Calculated Isotope Shifts $\Delta\nu_i = \nu_i(N_4^+) - \nu_i$ (in cm^{-1}) Obtained with the RCCSD-T PEF[b]

isotopes	$\Delta\nu_1$	$\Delta\nu_2$	$\Delta\nu_3$	$\Delta 2\nu_4$	$\Delta 2\nu_5$
$^{15}N^{14}N^{14}N^{14}N^+$	10.4	2.7	25.9	1.3	1.7
calcd[4]	11.2		25.2		
expt[4]	11.5[a]		24.8		
$^{14}N^{15}N^{14}N^{14}N^+$	11.3	4.3	26.9	3.1	1.7
calcd[4]	12.8		26.5		
expt[4]	12.6[a]		25.6		
$^{15}N^{15}N^{14}N^{14}N^+$	14.2	6.9	61.1	4.3	3.5
calcd[4]	16.4		60.1		
expt[4]	16.6[a]		58.7		
$^{15}N^{14}N^{15}N^{14}N^+$	37.6	7.1	37.0	4.5	3.3
calcd[4]	38.2		37.5		
expt[4]			36.9		
$^{15}N^{14}N^{14}N^{15}N^+$	35.6	5.5	37.0	2.6	3.3
calcd[4]	35.2		37.5		
expt[4]			36.9		
$^{14}N^{15}N^{15}N^{14}N^+$	39.6	8.6	37.1	6.4	3.3
calcd[4]	41.1		37.5		
expt[4]			36.9		
$^{15}N^{15}N^{15}N^{14}N^+$	49.7	11.3	63.9	7.7	4.9
calcd[4]	52.1		63.7		
expt[4]			62.5		
$^{15}N^{15}N^{14}N^{15}N^+$	47.3	9.7	64.3	5.7	5.0
calcd[4]	48.5		64.3		
expt[4]			62.9		
$^{15}N^{15}N^{15}N^{15}N^+$	75.9	13.9	74.8	9.0	6.6
calcd[4]	77.1		75.7		
expt[4]			74.4		

[a] The experimental difference is calculated from the calculated ν_1 of ref 4 for $^{14}N_4^+$. [b] The wavenumbers $\nu_i(^{14}N_4^+)$ are taken from Table 3.

In Table 3, the calculated anharmonic wavenumbers for the fundamental transitions of N_4^+ and the stretch harmonic force constants are compared with available experimental data. So far, only the ν_3 band origin has been determined to be 2234.5084 cm^{-1} in a gas-phase rotationally resolved spectrum.[5] The RCCSD-T value is larger by 4.8 cm^{-1}. The matrix value for ^{14}N ion has been observed[4] at 2237.6 cm^{-1}. For three asymmetric isotopomers, it was possible to detect also the ν_1 symmetric stretching fundamental.[4] Our calculated value of 2275.6 cm^{-1} is smaller than the value of 2282.6 calculated from the stretching harmonic force constants for the ^{14}N isotopomer.[4] For the asymmetric isotopomers, our theoretical values are smaller by 5−6 cm^{-1} than this experiment. From this comparison, we assume that the $1\nu_1$ band origin will lie probably a few wavenumbers lower than the calculated RCCSD-T value. On the basis of the harmonic force constants, the ν_2 wavenumber has been expected to lie between 344 and 480 cm^{-1}, in good agreement with our calculated value of 390.3 cm^{-1}. Using the RCCSD-T PEF, we have also calculated the harmonic stretch force constants in internal coordinates, which are compared in the same table with those derived in ref 4. The NN stretching constant is close to the value obtained from the matrix spectra. For both bending fundamentals, the wavenumbers are calculated to be very low in energy, with the ν_4 cis-bending at 90.7 cm^{-1} and the trans-bending at 133.8 cm^{-1}. In Table 3, we have included also the

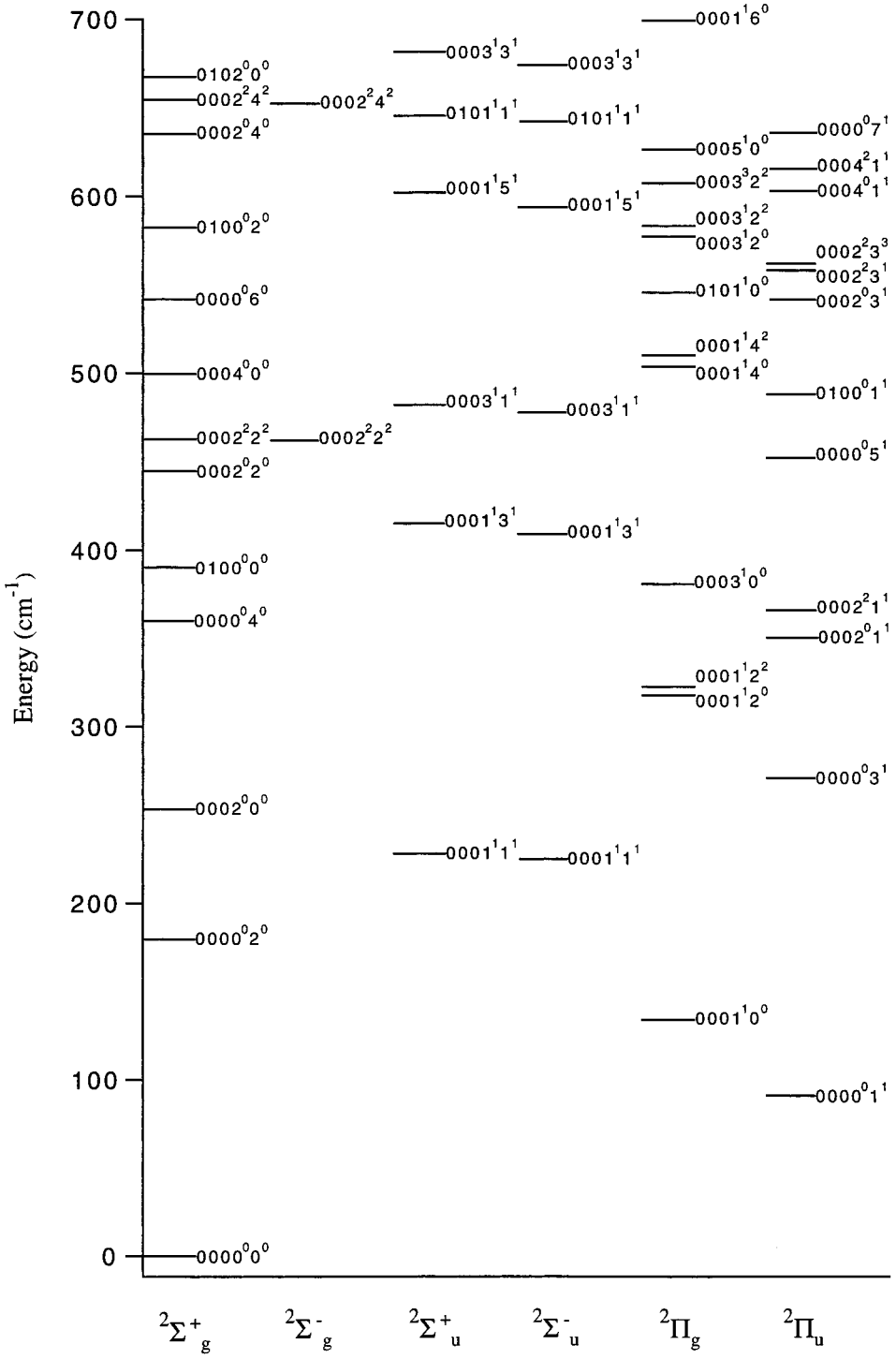

Figure 3. RCCSD-T energy levels of low lying vibrational modes in the electronic ground state of N_4^+.

harmonic wavenumbers calculated by Sohlberg[19] using the UHF method, which are less accurate that the present results. The comparison with the density functional results shows that both approaches describe the PEF for the bending modes correctly, but the stretching part is much less accurate.

In Table 4, the first rotational levels with $J = 1$ are given for all the fundamental vibrations. The *l*-doubling in the lowest $\nu_{4,5} = 1$ vibrational states of Π symmetry was calculated to be smaller than 0.001 cm^{-1} and is not quoted in the table.

Table 5 contains the anharmonic wavenumbers of the vibrational states for six symmetries obtained from the $J = 0$ and 1 variational calculations and their tentative assignments. As a result of the high density of bending and ν_2 states, these levels are given only up to about 700 cm^{-1}. They are also displayed in Figure 3. However, we have added some combination levels lying close to the antisymmetric streching mode, since the intensity of this mode will make such combination modes accessible spectroscopically and could yield, for the first time, an experimenatal information about the bending modes.

In Table 6, the isotope shifts for all fundamentals are compared with the matrix experiment.[4] The agreement can be considered as excellent for all isotopomers. For the ν_2, ν_4, and ν_5 fundamentals, the absolute shifts have been calculated to be much smaller than those for the ν_1 and ν_3 stretching modes.

The N_4^+ ion has been known to form clusters, such as N_4^+-Ar or $N_4^+(N_2)_n$.[9−11] In such complexes, the long-range parts of

TABLE 7: Calculated Quadrupole Moment[a] and Dipole Polarizability[b] (in a.u., for $R_1 = R_2 = 2.1$ and $R_3 = 3.8$ bohr) of N_4^+

Q_{xx}	Q_{zz}	Q_{RR}
−4.4705	8.9410	−31.5834

$\alpha_{\|}$	$\alpha_{\perp}$
77.694	13.532

[a] Using CEPA1, given with respect to the center of mass, and the *z* axis as a molecular axis. [b] Using the finite field approach and RCCSD-T.

the PEFs are dominated by the inductive interaction of the ionic charge with the dipole polararizabilities of the neutral species. Smaller contributions come from the induced dipoles with the dipole polarizability of N_4^+. To have some guidance about the long-range force caused by the ion, we have calculated its quadrupole moment using the CEPA-1 approach[32] and the finite field approach combined with the RCCSD-T method for the dipole polarizability. In additional calculations for N_2^+, we have compared both approaches with previous results calculated with larger AO basis set.[32] The comparison indicates that the values given for N_4^+ in Table 7 are probably somewhat too large, but we expect that the absolute values should be accurate to within about 10%.

6. Conclusions

Six-dimensional PEF for the $X^2\Sigma_u^+$ state of the N_4^+ ion has been generated and used in variational calculations of the rovibrational levels. The ion has three energetically low lying vibrational modes leading to a rather floppy structure. The combination levels with the symmetric and antisymmetric stretching modes calculated between 2200 and 3000 cm^{-1} should be accessible experimentally and would help to check the reliability of the bending part of the PEF. The quadrupole moment and the dipole polarizability of the ion can prove helpful in estimating the longe-range forces in clusters with N_4^+.

Acknowledgment. Financial support from the EEC as part of the TMR network Potential Energy Surfaces for Spectroscopy and Dynamics, Contract FMRX-CT96-088(DG12-BIUO), is gratefully acknowledged. S.C. and N.C.H. acknowledge financial support from the U.S. Office of Naval Research and the U.K. Leverhulme trust. C.L. thanks the Theoretical Chemistry Group at the University of Cambridge for a very stimulating stay.

References and Notes

(1) Payzant, J. D.; Kebarle, P. *J. Chem. Phys.* **1970**, *53*, 4723 and references therein.
(2) Ferguson, E. E. In *Kinetics of Ion−Molecule Reactions*; Ausloos, P., Ed.; Plenum: New York, 1979.
(3) Knight, L. B., Jr.; Johannessen, K. D.; Cobranchi, D. C.; Earl, E. A.; Feller, D.; Davidson, E. R. *J. Chem. Phys.* **1987**, *87*, 885.
(4) Thompson, W. E.; Jacox, M. E. *J. Chem. Phys.* **1990**, *93*, 3856.
(5) Ruchti, T.; Speck, T.; Connelly, J. P.; Bieske, E. J.; Linnartz, H.; Maier, J. P. *J. Chem. Phys.* **1996**, *105*, 2591 and references therein.
(6) Carnovale, F.; Peel, J. B.; Rothwell, R. G. *J. Chem. Phys.* **1988**, *88*, 642.
(7) Smith, G. P.; Lee, L. C. *J. Chem. Phys.* **1978**, *69*, 5393.
(8) Ostrander, S. C.; Weisshaar, J. C. *Chem. Phys. Lett.* **1986**, *129*, 220.
(9) Bieske, E. J. *J. Chem. Phys.* **1993**, *99*, 8672.
(10) Bieske, E. J. *J. Chem. Phys.* **1993**, *98*, 8573.
(11) Norword, K.; Luo, G.; Ng, C. Y. *J. Chem. Phys.* **1989**, *91*, 849.
(12) Conway, D. C. *J. Chem. Phys.* **1975**, *63*, 2219.
(13) Jarrold, M. F.; Illies, A. J.; Bowers, M. T. *J. Chem. Phys.* **1984**, *81*, 214.
(14) Schultz, R. H.; Armentrout, P. B. *J. Chem. Phys.* **1992**, *96*, 1046.
(15) de Castro, S. C.; Schaefer, H. F., III; Pitzer, R. M. *J. Chem. Phys.* **1981**, *74*, 550.
(16) Frecer, V.; Jain, D. C.; Sapse, A. M. *J. Phys. Chem.* **1991**, *95*, 9263.
(17) Sohlberg, K.; Futrell, J.; Szalewitz, K. *J. Chem. Phys.* **1991**, *94*, 6500.
(18) Langenberg, J. H.; Bucur, I. B.; Archirel, P. *Chem. Phys.* **1997**, *221*, 225.
(19) Sohlberg, K. *J. Mol. Struct. (THEOCHEM)* **1995**, *339*, 195.
(20) Deegan, M. J. O.; Knowles, P. J. *Chem. Phys. Lett.* **1994**, *227*, 321.
(21) Dunning, T. H. *J. Chem. Phys.* **1989**, *90*, 1007.
(22) Meyer, W. *J. Chem. Phys.* **1973**, *58*, 1017.
(23) MOLPRO is a package of ab initio programs written by H.-J. Werner and P. J. Knowles with contributions from J. Almlöf, R. D. Amos, M. J. O. Deegan, S. T. Elbert, C. Hampel, W. Meyer, K. Peterson, R. Pitzer, A. J. Stone, and P. R. Taylor.
(24) MOLDEN is a graphic package wirtten by G. Schaftenaar.
(25) Amos, R. D.; Alberts, I. L.; Andrews, J. S.; Colwell, S. M.; Handy, N. C.; Jayatilaka, D.; Knowles, P. J.; Kobayashi, R.; Laming, G. J.; Lee, A. M.; Maslen, P. E.; Murray, C. W.; Palmieri, P.; Rice, J. E.; Simandiras, E. D.; Stone, A. J.; Su, M.-D.; Tozer, D. J. *CADPAC6.0, The Cambridge Analytic Derivates Package*; Cambridge, UK, 1995.
(26) Stevens, P. J.; Devlin, F. J.; Chabalowski, C. F.; Frisch, M. J. *J. Phys. Chem.* **1994**, *98*, 11623.
(27) Hamprecht, F. A.; Cohen, A. J.; Tozer, D. J.; Handy, N. C. *J. Chem. Phys.*, in press.
(28) Strey, G.; Mills, I. M. *J. Mol. Spectrosc.* **1976**, *59*, 103.
(29) The PEFs and all results can be obtained by ftp to alpha.univ-mlv.fr under anonymous and your e-mail address.
(30) Bramley, M. J.; Handy, N. C.; Mills, I. M. *J. Mol. Spectrosc.* **1993**, *157*, 301.
(31) Huber, K. P.; Herzberg, G. *Constants of Diatomic Molecules*; Van Nostrand: 1979.
(32) Berning, A.; Werner, H.-J. *J. Chem. Phys.* **1994**, *100*, 1953.
(33) Hiraoka, K.; Nakajima, G. *J. Chem. Phys.* **1988**, *88*, 7709.